

Supporting Material

for

**Turn-on detection of Al³⁺ and Zn²⁺ ions by NSN donors probe:
Reversibility, logic gates and DFT calculations**

Sudhanshu Naithani^a, Nidhi Goswami^a, Sain Singh^b, Vikas Yadav^c, Sanjay Kumar^{d,e}, Pramod Kumar^f, Amit Kumar^{a*}, Tapas Goswami^{a*}, Sushil Kumar^{a*}

^a Department of Chemistry, Applied Science Cluster, University of Petroleum and Energy Studies (UPES), Dehradun-248007, Uttarakhand, India. Email: sushil.k@ddn.upes.ac.in

^b Department of Chemistry, Indian Institute of Technology Roorkee, 247667, Uttarakhand, India.

^c Nanoscopic Imaging and Sensing Lab, Indian Institute of Technology Delhi, Hauz Khas, New Delhi 110016, India.

^d Department of Chemistry, Muzaffarpur Institute of Technology, Muzaffarpur- 842003, India; ^e Department of Pharmacy, Muzaffarpur Institute of Technology, Muzaffarpur- 842003, India.

^f Department of Chemistry, Mahamana Malviya College Khekra (Baghpat), C.C.S. University Meerut, India.

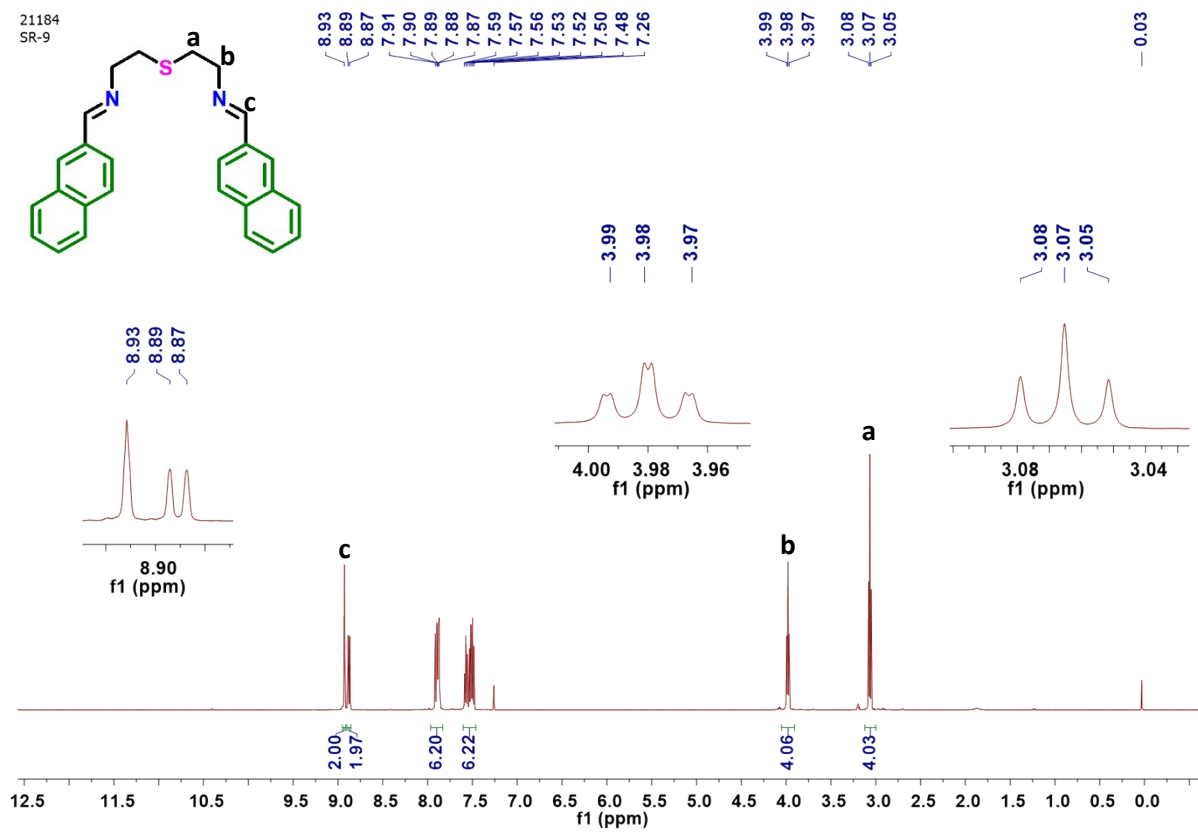


Fig. S1. ¹H NMR spectrum of NpSb in CDCl₃ at room temperature. ¹H NMR (CDCl₃, 500 MHz, TMS), δ (ppm): 8.93 (s, 2H, -CH=N-), 8.89 (m, 2H), 7.89 (m, 6H), 7.59-7.48 (m, 6H), 3.98 (t, 4H, -CH₂-N-), 3.07 (t, 4H, -CH₂-S<).

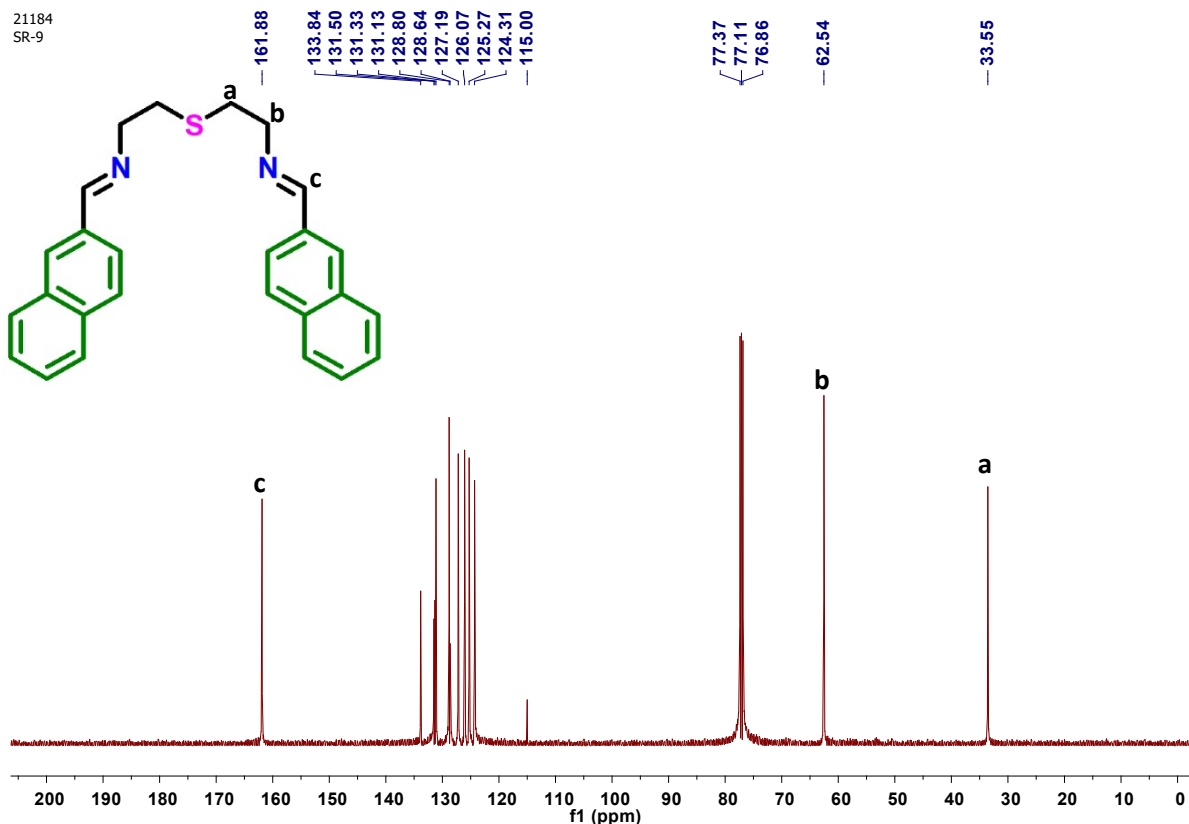


Fig. S2. ^{13}C NMR spectrum of NpSb in CDCl_3 at room temperature. ^{13}C NMR (CDCl_3 , 500 MHz), δ (ppm): 161.88, 133.84, 131.50, 131.33, 131.13, 128.80, 128.64, 127.19, 126.07, 125.47, 124.31, 115.00, 62.54, 33.55.

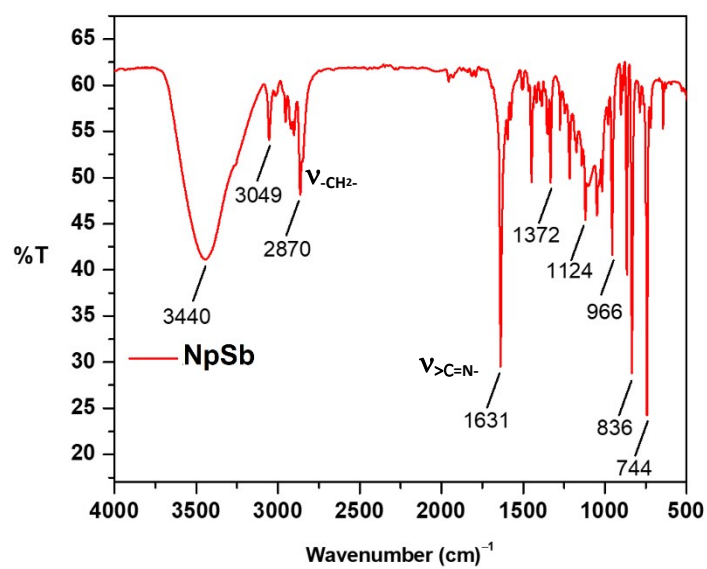


Fig. S3. FT-IR spectrum of **NpSb**. IR data (KBr disk, cm^{-1}): 3440, 3049, 2870, 1631 ($\nu_{\text{C}=\text{N}}$), 1372, 1124, 966, 836, 744.

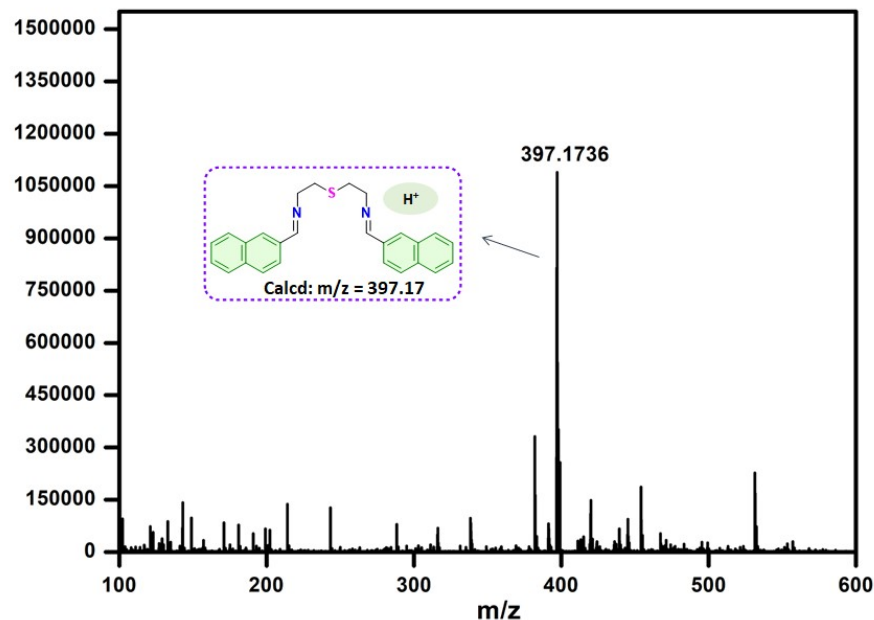


Fig. S4. ESI-MS analysis of probe **NpSb** in methanol at room temperature.

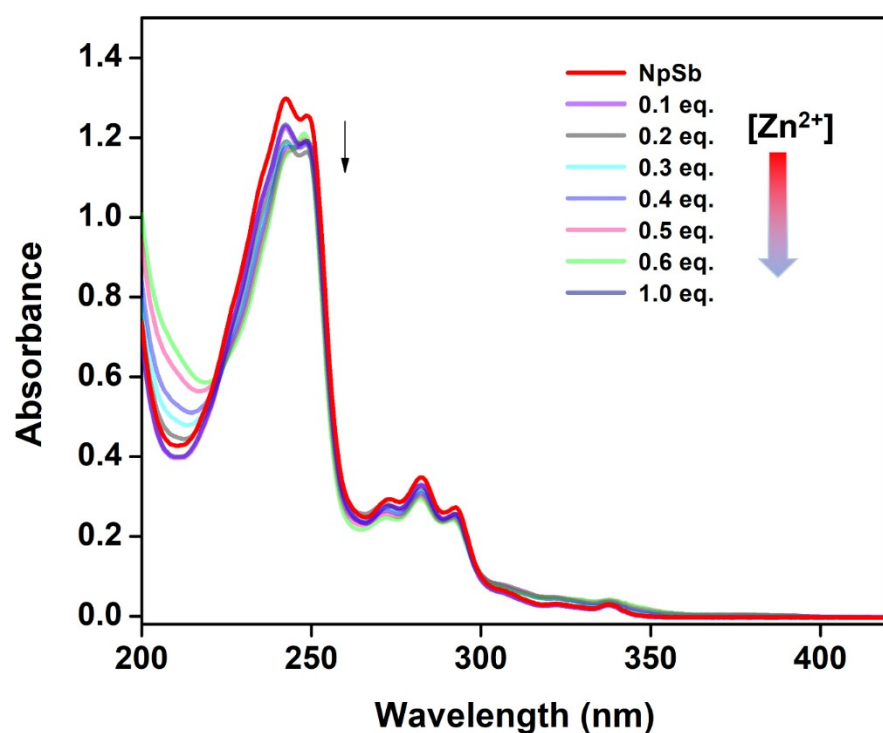


Fig. S5. UV-Vis spectral changes for **NpSb** (1.0×10^{-5} M) in $\text{CH}_3\text{CN}-\text{H}_2\text{O}$ (4:1, v/v) after successive addition of Zn^{2+} ions (0-1.0 equiv.).

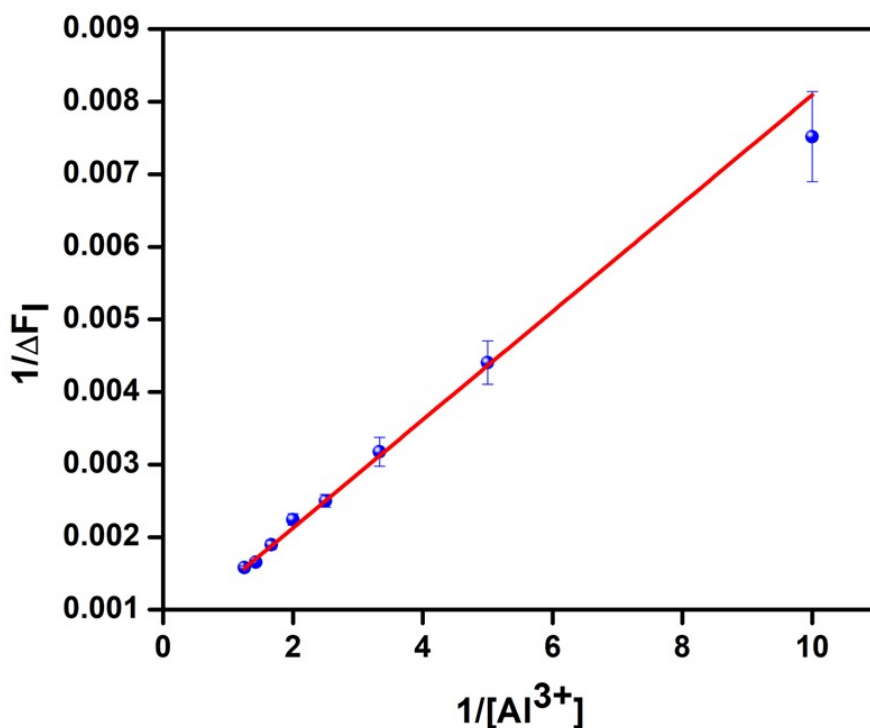


Fig. S6. Determination of binding constant of **NpSb** for Al^{3+} by employing Benesi-Hildebrand plots from fluorescence spectroscopy.

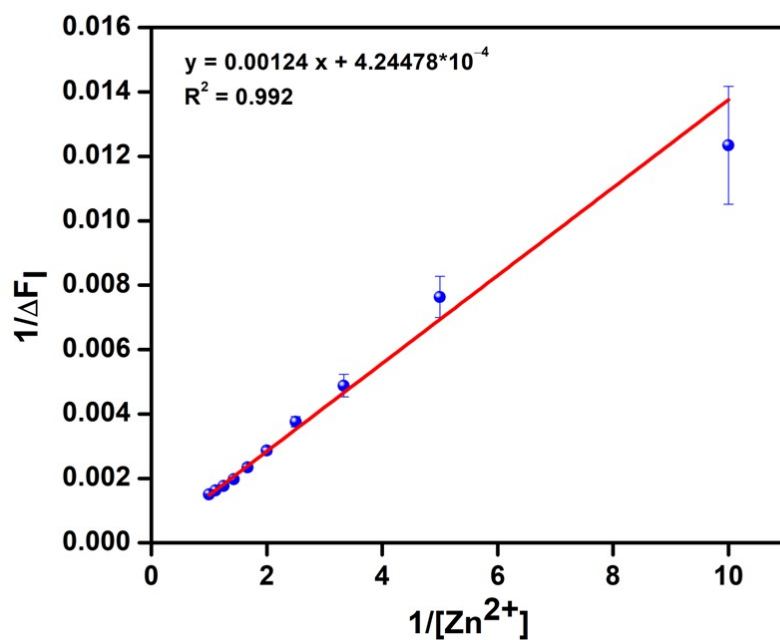


Fig. S7. Determination of binding constant of **NpSb** for Zn^{2+} by employing Benesi-Hildebrand plots from fluorescence spectroscopy.

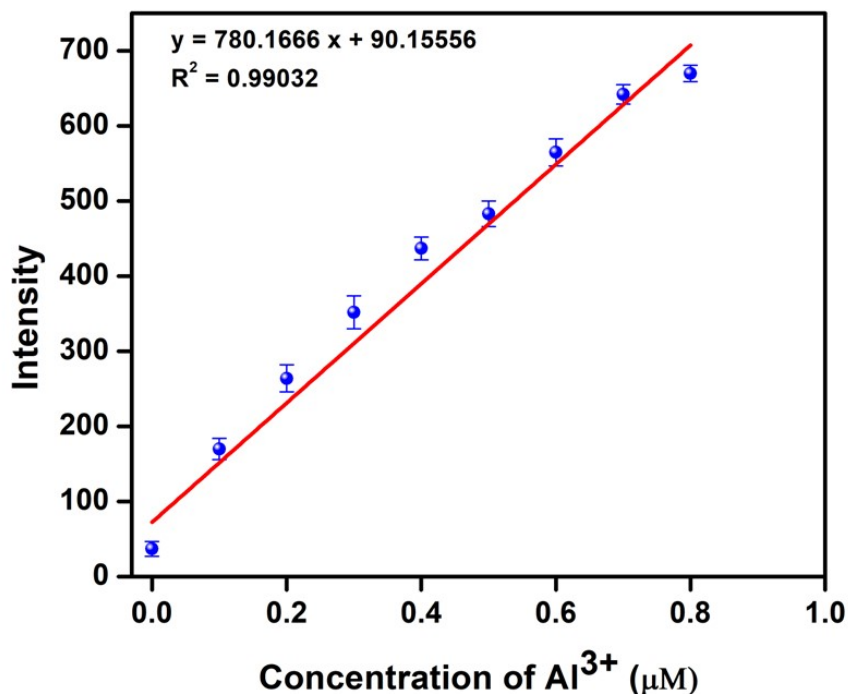


Fig. S8. Linear curves of the emission intensity of **NpSb** with Al^{3+} for the determination of LoD in CH_3CN-H_2O (4:1, v/v).

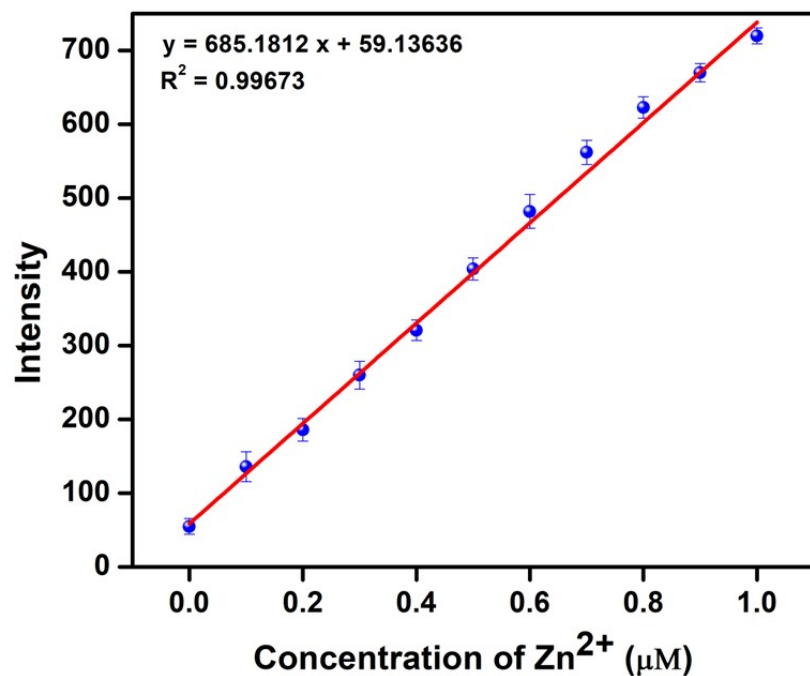


Fig. S9. Linear curves of the emission intensity of **NpSb** with Zn^{2+} for the determination of LoD in CH_3CN-H_2O (4:1, v/v).

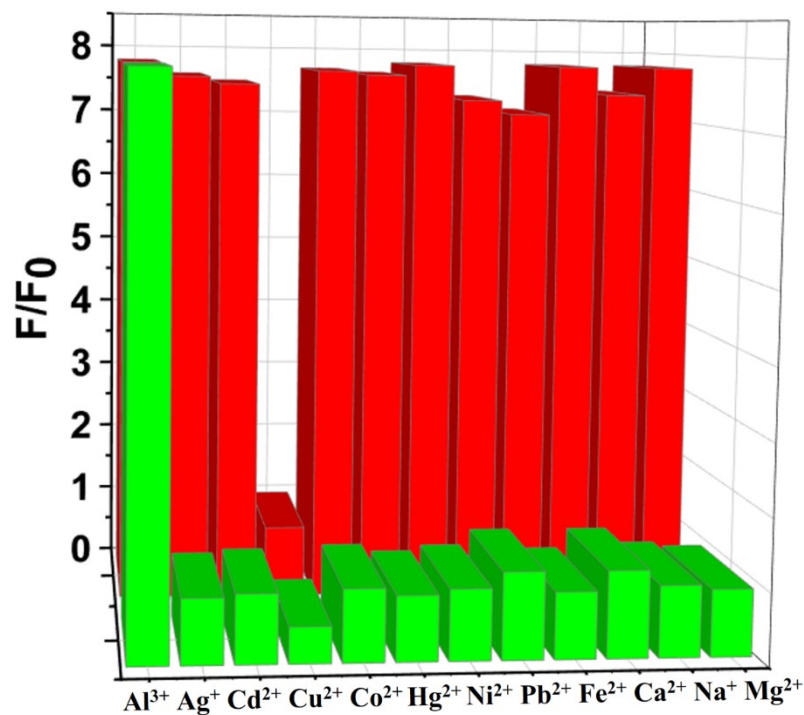


Fig. S10. Relative fluorescence Intensity of **NpSb** with Al^{3+} in the presence of 10 equiv of other cations in CH_3CN-H_2O (4:1, v/v).

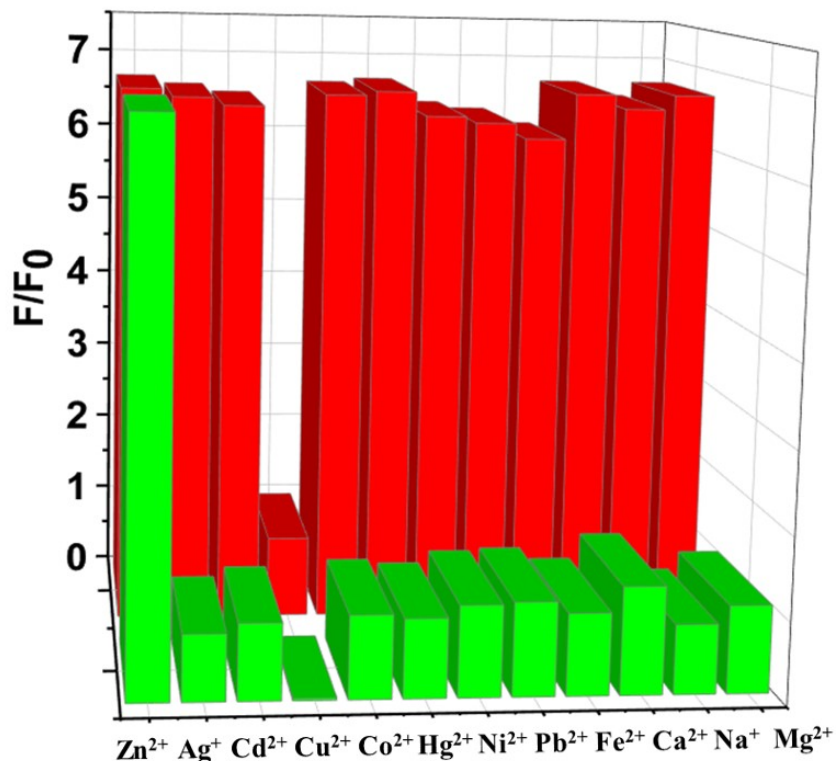


Fig. S11. Relative fluorescence intensity of **NpSb** with Zn^{2+} in the presence of 10 equiv of other cations in CH_3CN-H_2O (4:1, v/v) solution.

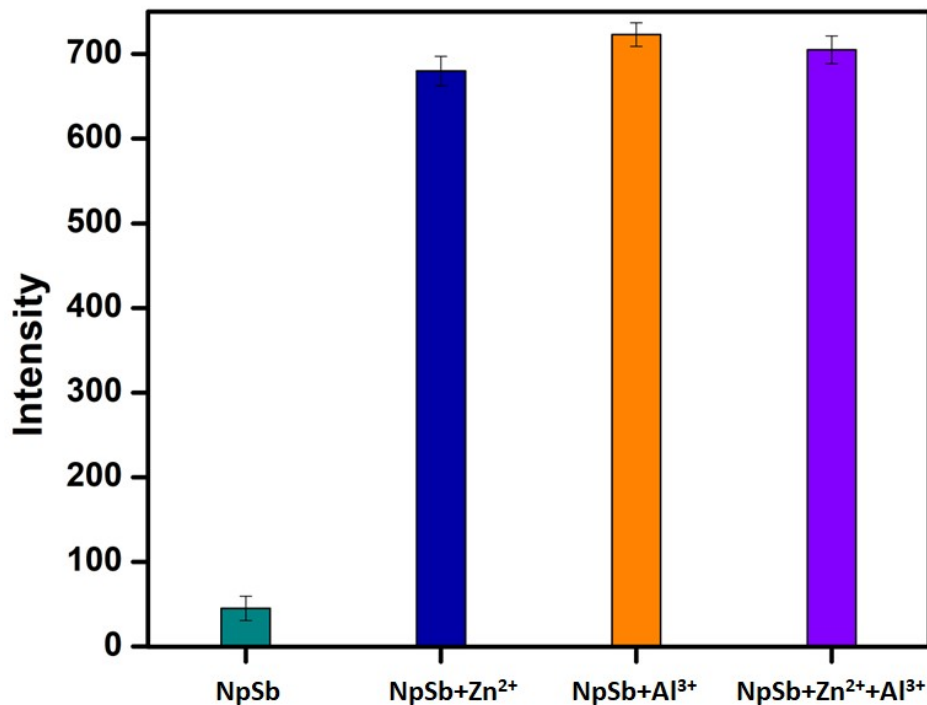


Fig. S12. Fluorescence Intensity of **NpSb** with Al^{3+} and Zn^{2+} in CH_3CN-H_2O (4:1, v/v) solution.

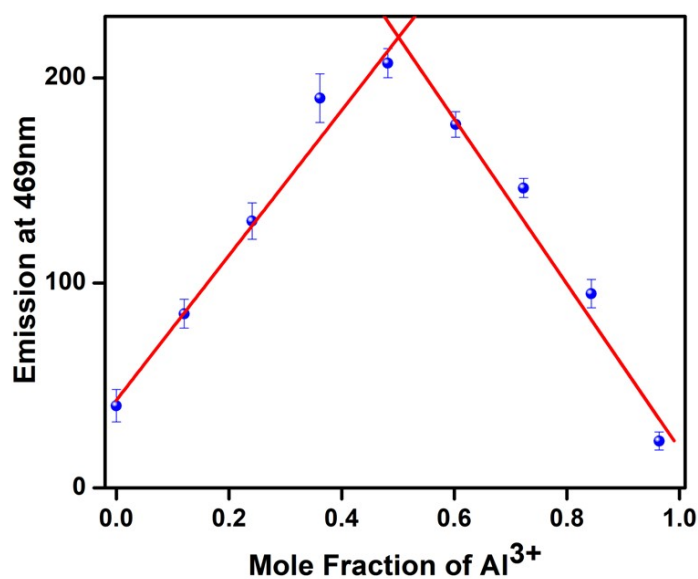


Fig. S13. Job's Plot analyses for **NpSb** vs. Al^{3+}

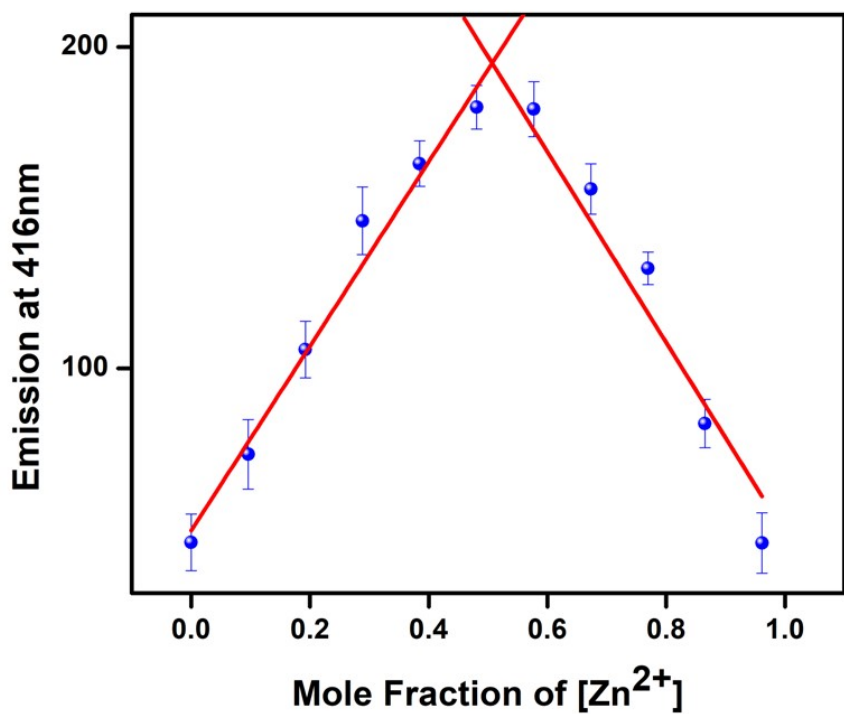


Fig. S14. Job's Plot analyses for NpSb vs. Zn^{2+}

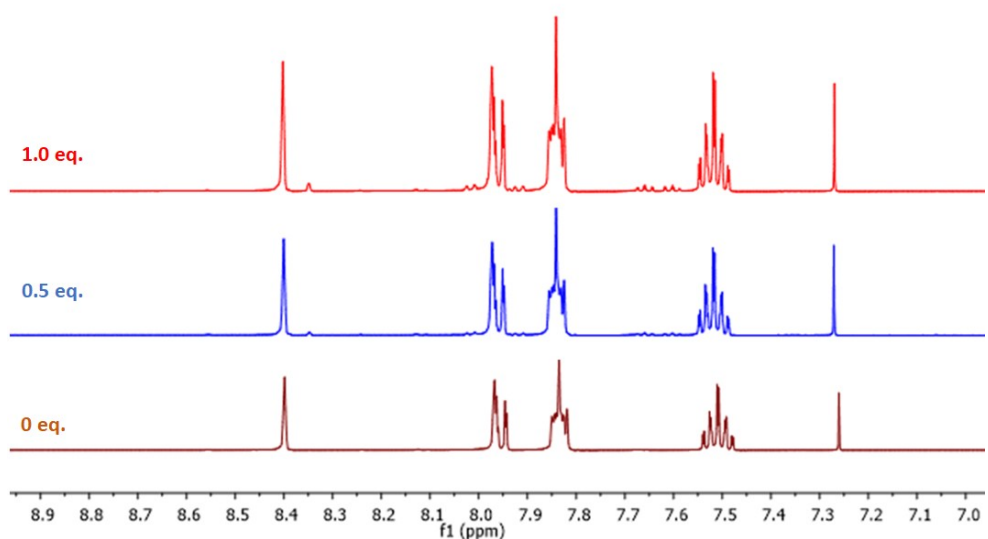


Fig. S15. ^1H NMR spectra of NpSb when treated with Zn^{2+} ions.

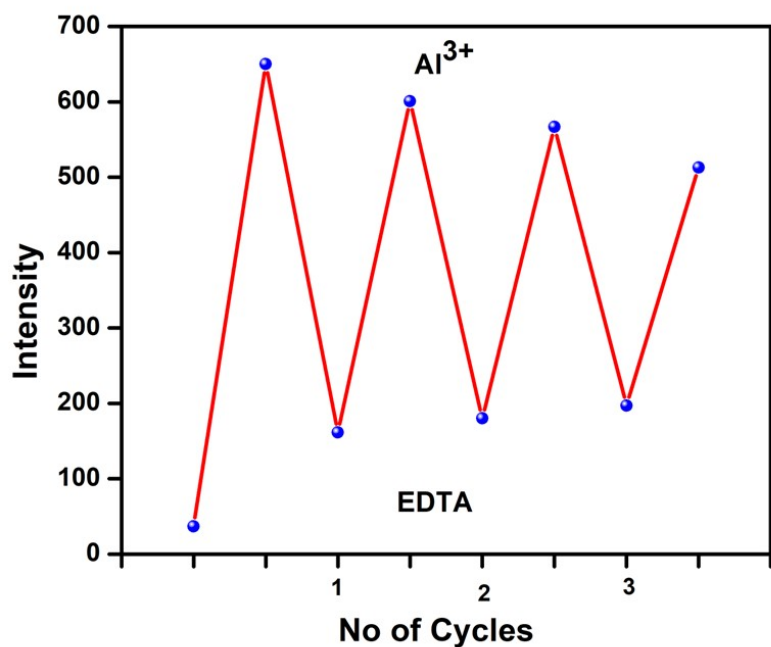


Fig. S16. Emission intensity of NpSb after the alternate addition of Al³⁺ and EDTA.

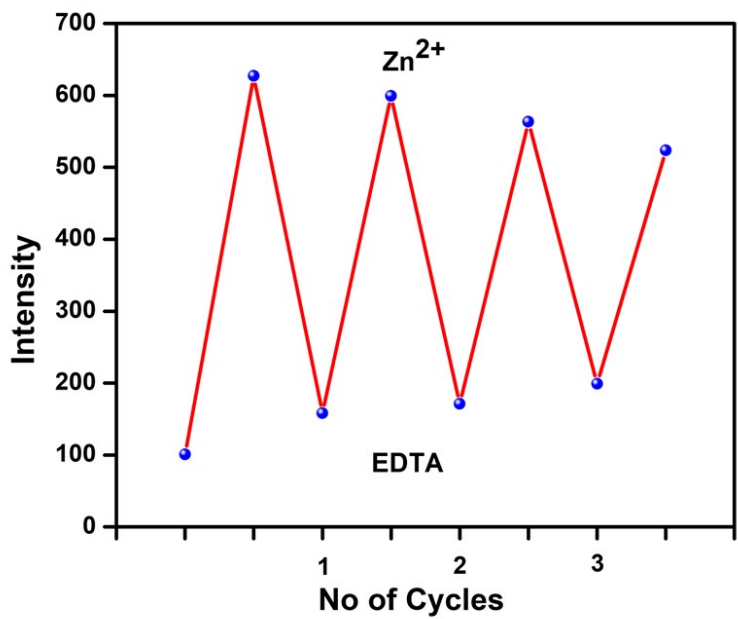


Fig. S17. Emission intensity of NpSb after the alternate addition of Zn²⁺ and EDTA.

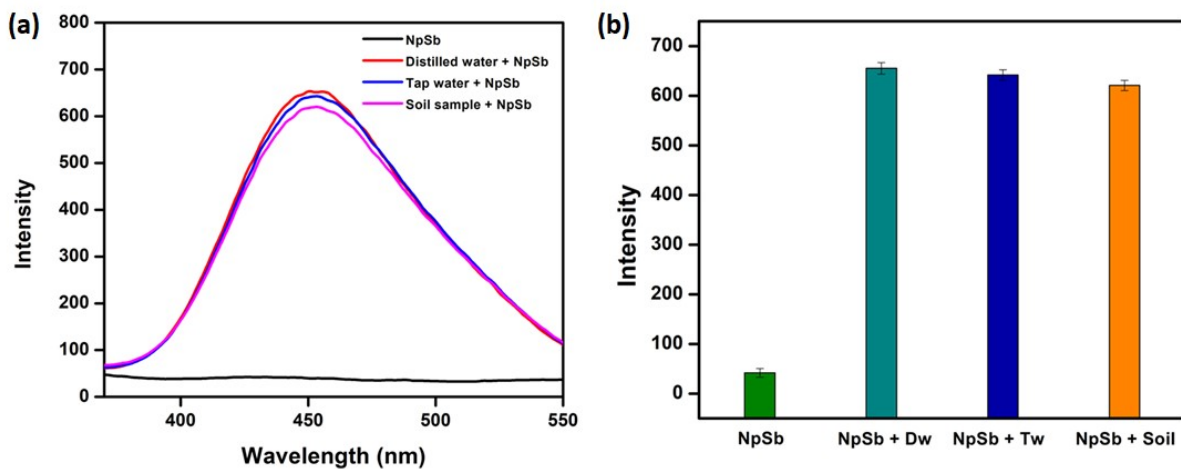


Fig. S18. Interaction of probe **NpSb** with real samples (distilled water, tap water and soil sample) spiked with 2.0 equiv of Al³⁺ ions. (Dw = distilled water; Tw = tap water).

Calculation of Quantum Yield.

The fluorescence quantum yield (Φ) was calculated via integration of the area under fluorescence curve using equation.

$$\Phi_{\text{sample}} = \frac{\Phi_{\text{ref}} \times \frac{OD_{\text{ref}} \times A_{\text{sample}} \times \zeta_{\text{sample}}}{OD_{\text{sample}} \times A_{\text{ref}} \times \zeta_{\text{ref}}}}{}$$

Where, OD = Optical density,

ζ = Refractive indices of solvent

A= Area under the curve

The standard use for the calculation was anthracene (0.27 in ethanol) with excitation at 340nm.

Table S1. Crystallographic data for **NpSb**.

Formula	C ₂₆ H ₂₄ N ₂ S
Formula weight (gmol ⁻¹)	396.53
Space group (hall)	-P 2yn
Temperature/K	150(2)
λ (Å) (Cu-K α)	1.54184
Crystal system	monoclinic
a (Å)	5.7751(6)
b (Å)	46.275(3)
c (Å)	7.7780(8)
α (°)	90
β (°)	90.655(10)
γ (°)	90
V (Å ³)	2078.5(3)
Z	4
ρ_{calc} (gcm ⁻³)	1.267
Crystal size (mm)	0.18 × 0.15 × 0.10
$F(000)$	840
Index ranges	-7 < h < 7 -56 < k < 56 -9 < l < 9
Reflns/ para/ restraints.	3889/263/407
GOF on F^2	1.119
$R1^a$ [$I > 2\sigma(I)$]	0.1178
$R1$ [all data]	0.1694
$wR2^b$ [$I > 2\sigma(I)$]	0.3025
$wR2$ [all data]	0.3474

^aR1= $\Sigma ||\text{Fo}|-|\text{Fc}||/\Sigma |\text{Fo}|$; ^bwR2= $[\sum w(|\text{Fo}|^2 - |\text{Fc}|^2)] / \sum w(\text{Fo})^2$

Table S2. Selected bond lengths [Å] and angles [°] in the single crystals of **NpSb**.

Bond Length (Å)	Bond Angle (°)		
S(1)–C(13)	1.784(10)	C(13)–S(1)–C(14)	101.7(5)
S(1)–C(14)	1.803(9)	C(12)–C(13)–S(1)	112.6(7)
C(13)–C(12)	1.510(13)	C(15)–C(14)–S(1)	112.6(6)
C(14)–C(15)	1.510(13)	C(15)–N(2)–C(16)	116.1(8)
C(12)–N(1)	1.477(12)	C(11)–N(1)–C(12)	116.0(10)
C(15)–N(2)	1.478(11)		
C(11)–N(1)	1.263(12)		
C(16)–N(2)	1.257(11)		

Table S3. Detection of Al³⁺ in real samples.

Tap water	Al³⁺ added (μM)	Al³⁺ calculated (μM)	% Recovery
	0.3	0.28	93.3
	0.8	0.77	96.2
Distilled water			
	0.3	0.29	96.6
	0.8	0.83	103.7
Soil sample			
	0.3	0.31	103.3
	0.8	0.81	98.7